geoconvention
Virtual Event
September 13 - 15
2021

Tensile radiation from slip on rough fractures

Scott Leaney
SLRDC

Summary

Tensile components are often observed in tectonic and hydraulically induced earthquakes, leading to a variety of interpretations and conjecture as to underlying causes. In this paper a simple extension to the model of slip on a planar fracture is studied wherein texture or roughness is added to the fracture via coupled excess compliances. This reasonable extension of a purely planar fracture model leads to media with triclinic symmetry, even though the background medium may be isotropic. Moment tensors that have pure in-fracture-plane slip, built in an effective medium with coupled excess fracture compliances are analyzed by extracting the opening angle from the eigenvalues. The consequence of pure slip along a fracture plane with roughness is that moment tensors with tensile components are produced. It is conjectured that fracture surface roughness may be a simple explanation for some observed tensile components.

Introduction

The properties of source moment tensors in anisotropic media have been studied (Vavryčuk, 2005; Leaney and Chapman, 2010; Grechka, 2020), but as far as we know, moment tensors have not been studied in the context of a coupled excess compliance (CEC) fracture model. In what follows we review the theory behind the construction of a stiffness tensor that is long wavelength -equivalent to a medium with generalized fractures as defined by a 3x3 excess fracture compliance matrix. Bounds are given for off-diagonal elements and a modified form of normalized weakness parameters is proposed. Moment tensors are then constructed by contracting the stiffness tensor with a potency tensor defined by pure in-fracture-plane slip. The opening angle is extracted from the eigenvalues of the moment tensor to quantify the tensile component and comparative radiation patterns are shown.

A fractured medium with coupled excess compliances

We wish to study the case where the stiffness tensor $\boldsymbol{c}$ is composed of a background medium with a single set of vertical fractures. Using linear slip theory (Schoenberg, 1980) showed that the long wavelength effective medium stiffness matrix can be constructed by summing compliance matrices and inverting back to stiffness. Given a background medium compliance matrix, $\boldsymbol{s}_b$, an arbitrary number of non-interacting, long wavelength-equivalent fractures, each with compliance matrix $\boldsymbol{s}_f$, can be added to obtain the equivalent medium stiffness matrix (Grechka and Tsvankin, 2003):

$$\boldsymbol{c}_e = \boldsymbol{s}_e^{-1} = \left[\boldsymbol{s}_b + \sum \boldsymbol{s}_f\right]^{-1} = \left[\boldsymbol{c}_b^{-1} + \sum \boldsymbol{s}_f\right]^{-1}. \quad (1)$$

The long-wavelength equivalent fracture of a single set of parallel fractures may be represented by a 3x3 compliance matrix (Schoenberg and Douma, 1988), $\boldsymbol{Z}$:

$$\boldsymbol{Z} = \begin{pmatrix} Z_N & Z_{NV} & Z_{NH} \\ Z_{NV} & Z_V & Z_{VH} \\ Z_{NH} & Z_{VH} & Z_H \end{pmatrix}, \tag{2}$$

where *N*=normal, *V*=vertical shear and *H*=horizontal shear and the off-diagonal terms signify displacements due to stresses and vice versa. For example, Z_{NV} means the vertical shear displacement due to a normal stress or the normal displacement due to a vertical shear stress. Following convention, the diagonal terms do not appear as Z_{NN}, etc., but rather as Z_N.

The excess compliance of a single set of vertical fractures as described by (2) with normals parallel to the x_1-axis has a compliance matrix of the form (e.g. Grechka et al., 2003):

$$s_f = \begin{pmatrix} Z_N & 0 & 0 & 0 & Z_{NV} & Z_{NH} \\ 0 & 0 & 0 & 0 & 0 & 0 \\ 0 & 0 & 0 & 0 & 0 & 0 \\ 0 & 0 & 0 & 0 & 0 & 0 \\ Z_{NV} & 0 & 0 & 0 & Z_V & Z_{VH} \\ Z_{NH} & 0 & 0 & 0 & Z_{VH} & Z_H \end{pmatrix}. \tag{3}$$

Each fracture set defined by (3) may be rotated and included in the summation in (1), but for our purposes a single vertical fracture set defined by (3) without rotation will be used.

A brief review of coupled compliance fracture theory follows. Schoenberg and Douma (1988) referred to *micro-corrugated* fractures, describing fractures with a non-zero off-diagonal element (Z_{NV} or Z_{NH}) in (2) as *monoclinic* fractures and another case with a non-zero coupled shear term (Z_{VH}) as *orthorhombic* fractures. Figure 1 shows the idea of a vertical fracture with micro-corrugations schematically. We refer to such fractures as being *rough* or having *texture*. Note that Figure 1 portrays 2D fractures that extend indefinitely out of the plane in the $\boldsymbol{x_2}$ direction. 3D fractures with general roughness have a complete $\boldsymbol{Z}$ matrix and as will be shown below, produce triclinic symmetry.

Grechka and Tsvankin (2003) developed a classification based on the structure of the fracture compliance matrix (2), distinguishing between diagonal (*DI*) fractures and simpler, rotationally invariant (*RI*) fractures. *DI* fractures have $Z_{NV} = Z_{NH} = 0$ but may have $Z_{VH} \neq 0$, as an angle α, where $2\alpha = \tan^{-1}[2Z_{VH}/(Z_V - Z_H)]$, can be used to zero out this term. *RI* fractures have the additional property that $Z_{VH} = 0$ and $Z_V = Z_H$. *RI* fractures were considered by Schoenberg and Sayers (1995), while those considered by Schoenberg and Helbig (1997) were a special case of *DI* fractures with $Z_{VH} = 0$. Grechka and Tsvankin (2003) call the general form of a fully populated fracture compliance matrix "*Gn*".

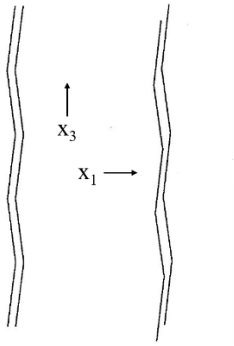

Figure 1. Schematic for 2D micro-corrugated or rough fractures with orthorhombic (left) and monoclinic (right) symmetry. (Adapted from Schoenberg and Douma, 1988).

Fractures with a non-zero NV coupled compliance term were studied by Bakulin et al. (2000), who gave expressions for the resulting monoclinic stiffness tensor when the fractures were vertical and the background medium isotropic. Grechka and Tsvankin (2003) gave the general case formulas for the 21 compliance moduli of a single fracture set with arbitrary dip and azimuth. They studied the invertibility for fracture parameters from minimum measurement sets. Grechka et al. (2003) studied the inverse problem for vertical fractures given data of NMO ellipses, split-shear slownesses and multi-azimuthal walkaway VSP slownesses. Fuck and Tsvankin (2006) studied the case of orthogonal fracture sets with general compliance coupling terms and found that terms depending on Z_{NH} were the most significant for azimuthal P-wave AVAz. Minato et al. (2020) included a compliance coupling term in 2D modelling of single well imaging data and inverted using least-squares migration.

While non-zero coupling terms have been considered in a few modelling studies, the magnitudes of these terms are largely unknown and ad hoc values have been assigned. Hood and Schoenberg (1995) used a value $Z_{NV} = 0.10$, being 10% of the value of Z_N; Fuck and Tsvankin (2006) used similar values. The only mathematical constraint is a stability condition so that $Z_{IJ}^2 \leq Z_I Z_J$, for $I,J = N,V,H$ to ensure non-negative definiteness of the fracture compliance matrix (2). Thus, the off-diagonal compliances, Z_{IJ}, may be negative. Nakagawa et al. (2000) proposed a coefficient to quantify coupling as $R_{IJ} = \sqrt{Z_{IJ}Z_{JI}}/\sqrt{Z_I Z_J}$. Due to elastic reciprocity, $Z_{JI} = Z_{IJ}$, and this was verified experimentally by Nakagawa et al. (2000). Thus, $Z_{IJ} = R_{IJ}\sqrt{Z_I Z_J}$ is a useful relation to define the off-diagonal coupling terms, with $|R_{IJ}| < 1$.

Grechka et al. (2003) defined normalized weakness parameters for an isotropic background by using the geometric mean of bulk and shear stiffnesses for the coupling terms. These parameters were then used in a weak anisotropy approximation. Here we propose a modification to those parameters for the case of a VTI background following from the definitions of Schoenberg and Helbig (1997). Including the diagonal parameters, the complete set of fracture weakness parameters is

$$\delta_N = \frac{C_{11}Z_N}{1 + C_{11}Z_N}, \delta_V = \frac{C_{44}Z_V}{1 + C_{44}Z_V}, \delta_H = \frac{C_{66}Z_H}{1 + C_{66}Z_H},$$

$$\delta_{NV} = \frac{\sqrt{C_{11}C_{44}}Z_{NV}}{1+\sqrt{C_{11}C_{44}}|Z_{NV}|}, \delta_{NH} = \frac{\sqrt{C_{11}C_{66}}Z_{NH}}{1+\sqrt{C_{11}C_{66}}|Z_{NH}|}, \delta_{VH} = \frac{\sqrt{C_{44}C_{66}}Z_{VH}}{1+\sqrt{C_{44}C_{66}}|Z_{VH}|}. \quad (4)$$

As an example of a stiffness tensor with CEC fractures, a VTI background medium is used (Vp=4km/s, Vs=2.2km/s, density=2.5) with Thomsen parameters $(\varepsilon, \delta, \gamma) = (0.28, 0.13, 0.22)$. Together with a fracture compliance matrix given by the parameter set: $(Z_N, Z_V, Z_H, Z_{NV}, Z_{NH}, Z_{VH}) = 10^{-2}(1.39, 1.74, 1.74, -0.621, -0.621, -0.694)$ as in (3). These values come from $R_{IJ} = -0.4$ or 40% of the maximum allowed under non-negative definiteness (Minato et al. (2020) used 50%). The normalized weakness set for this model is: $(\delta_N, \delta_V, \delta_H, \delta_{NV}, \delta_{NH}, \delta_{VH}) = (0.454, 0.174, 0.247, -0.201, -0.265, -0.117)$. The resulting stiffness tensor for this *Gn* effective medium is shown below for an isotropic background in equation (5). It has 16 non-zero moduli and has triclinic symmetry (Grechka et al., 2003). Thus, a single vertical fracture set with roughness can produce a very general type of anisotropic medium. Details behind the values for the excess compliance matrix, $\boldsymbol{Z}$, used to construct $\boldsymbol{c}_e$, are given later.

$$\boldsymbol{c}_e^{ISO} = \begin{pmatrix} 10.53 & 4.16 & 4.16 & 0 & 0.741 & 0.741 \\ 4.16 & 15.15 & 6.01 & 0 & 0.293 & 0.293 \\ 4.16 & 6.01 & 15.15 & 0 & 0.293 & 0.293 \\ 0 & 0 & 0 & 4.84 & 0 & 0 \\ 0.741 & 0.293 & 0.293 & 0 & 4.08 & 0.361 \\ 0.741 & 0.293 & 0.293 & 0 & 0.361 & 4.08 \end{pmatrix}. \quad (5)$$

Equation (5) shows repeated values, for example, c25=c35=0.293. This is due to the simplicity of the isotropic background. The same fracture set in a VTI background with the aforementioned Thomsen parameters produces the effective medium stiffness matrix shown in equation (6).

$$\boldsymbol{c}_e^{VTI} = \begin{pmatrix} 13.54 & 4.99 & 4.65 & 0 & 0.931 & 1.290 \\ 4.99 & 22.57 & 6.91 & 0 & 0.344 & 0.476 \\ 4.65 & 6.91 & 14.77 & 0 & 0.320 & 0.443 \\ 0 & 0 & 0 & 4.840 & 0 & 0 \\ 0.931 & 0.344 & 0.320 & 0 & 4.091 & 0.487 \\ 1.290 & 0.476 & 0.443 & 0 & 0.487 & 5.86 \end{pmatrix}. \quad (6)$$

Having constructed a stiffness tensor for an effective medium with a single set of rough fractures, it will now be used in the construction of a moment tensor.

Moment tensors with coupled fracture compliance

An earthquake source is commonly represented by a symmetric moment tensor (Burridge and Knoppoff, 1964). The symmetric moment tensor, $\boldsymbol{M}$, has six independent elements and may be constructed in general anisotropic media using (Chapman and Leaney, 2012):

$$\boldsymbol{M} = \widetilde{\boldsymbol{M}}_{iso} + \boldsymbol{c}: (\widehat{\boldsymbol{d}}\widehat{\boldsymbol{n}} + \widehat{\boldsymbol{n}}\widehat{\boldsymbol{d}})A[d]/2, \quad (7)$$

where $\widetilde{\boldsymbol{M}}_{iso}$ is a purely diagonal term representing isotropic pressure change, $\boldsymbol{c}$ is the stiffness tensor at the source, the colon symbol (:) means contraction over two dimensions between

tensors, $\hat{\boldsymbol{d}}$ and $\hat{\boldsymbol{n}}$ are unit displacement (slip) and fault normal vectors, respectively, and $A[d]$ is the area times total displacement. The term to the right of ":" has been called the *source tensor* (Vavryčuk, 2005), or the *potency tensor* (Ben Zion, 2001), denoted by $\boldsymbol{D}$ with scalar potency $D = A[d]$. The form of the *source tensor* has been utilized as a constraint in moment tensor interpretation (Grechka et al., 2017), but without $\widetilde{\boldsymbol{M}}_{iso}$, equation (6) is an incomplete description of a moment tensor as it requires only five parameters for its representation. The reason for the tilde is that the second term may also give rise to a diagonal (isotropic) part of $\boldsymbol{M}$ if $\hat{\boldsymbol{d}}$ and $\hat{\boldsymbol{n}}$ are not orthogonal. That is, if $\hat{\boldsymbol{d}} \cdot \hat{\boldsymbol{n}} = \sin\chi \neq 0$ then there is an opening / closing of the fault and the moment tensor is said to have a tensile component. The opening angle is simply determined from the eigenvalues of $\boldsymbol{M}$ or $\boldsymbol{D}$ as (Vavryčuk, 2005):

$$sin\chi = (\Lambda_1 + \Lambda_3)/(\Lambda_1 - \Lambda_3), \tag{8}$$

where the eigenvalues have been sorted ($\Lambda_1 > \Lambda_2 > \Lambda_3$). If the medium is isotropic then the opening angle will be the same for both $\boldsymbol{M}$ or $\boldsymbol{D}$, but if the source medium as represented by $\boldsymbol{c}$ is anisotropic, then even a pure slip source with $\chi = 0$ can produce false tensile components (Vavryčuk, 2005; Leaney and Chapman, 2010; Grechka, 2020). Moment tensor decompositions have been developed so that the true slip and opening angles can be recovered from the source tensor (Vavryčuk, 2005) or from the complete moment tensor (Chapman and Leaney, 2012).

The exact expression for $\widetilde{\boldsymbol{M}}_{iso} = \widetilde{M}_{iso}\boldsymbol{I}$ in (7) has been derived for general anisotropic media, as well as a linearized approximation: $\widetilde{M}_{iso} = \kappa[V] = V'[P]$ (Chapman and Leaney, 2012), where κ is the effective anisotropic bulk modulus and $[V]$ is the volume change due to a pressure change $[P]$ in an effective spherical volume V'. In what follows, we will consider only moment tensors constructed with $\widetilde{M}_{iso} = 0$ and $\chi = 0$. In other words, we consider simple sources with pure in-plane slip and no additive isotropic components. Our interest here is solely in the role of $\boldsymbol{c}$, the stiffness tensor at the source, and in a very limited class of model for $\boldsymbol{c}$, as described in the previous section. In the absence of any $\widetilde{\boldsymbol{M}}_{iso}$ component, the moment tensor may be written simply as $\boldsymbol{M} = \boldsymbol{c}\colon\boldsymbol{D}$ and the source tensor recovered as $\boldsymbol{D} = \boldsymbol{s}\colon\boldsymbol{M}$, where $\boldsymbol{s} = \boldsymbol{c}^{-1}$ is the compliance matrix of the elastic medium at the source. In the next section we examine the recovered opening angle (tensile component) determined from (8), using a VTI background source medium and selected parameters to define $\boldsymbol{Z}$ that produced the stiffness tensor in equation (6).

Moment tensor modelling results

We now construct a moment tensor for a pure in-fracture-plane slip source in an effective fractured medium with compliance coupling to represent fracture roughness. The fracture compliance matrix used to build the stiffness matrix (6) was built as follows. The fast / slow shear wave splitting velocity ratio was set to 0.10, defining c_{55} from c_{44} and hence the vertical shear fracture compliance $Z_V = 1/c_{55} - 1/c_{44}$ (Hood, 1991). Z_N is obtained from the compliance ratio $Z_N/Z_V = 0.8$ as representing gas-filled fractures; Z_H is obtained from $Z_H/Z_V = 1$. Coupling parameters were set such that all coupling coefficients $R_{IJ} = -0.40$, which yielded the normalized fracture weakness parameters given previously. The source tensor $\boldsymbol{D}$ was formed following the flow described by Leaney (2014), in this case defining the slip direction vector, $\hat{\boldsymbol{d}}$, to be purely horizontal and in the plane of the fracture; left-lateral strike-slip in the N-S direction. It has been

found that off-diagonal excess compliance coupling terms need to be negative to produce positive opening angles. Equations (9) show the normalized moment tensors for planar and rough fractured media. In the case of the planar medium, it is a DI orthorhombic medium parameterized as by Schoenberg and Helbig (1997).

$$\boldsymbol{M}_{planar} = \begin{pmatrix} 0 & 1 & 0 \\ 1 & 0 & 0 \\ 0 & 0 & 0 \end{pmatrix} \qquad \boldsymbol{M}_{rough} = \begin{pmatrix} 0.216 & 0.982 & 0.081 \\ 0.982 & 0.079 & 0 \\ 0.081 & 0 & 0.074 \end{pmatrix} \tag{9}$$

The opening angle for $\boldsymbol{M}_{rough}$ is $3.9°$, corresponding to an opening/slip ratio of about 1/15, being close to values found by Vavryčuk (2011) in the analysis of regional earthquakes. This demonstrates that slip along rough fractures, when modelled using an effective medium theory as described above, can produce a significant tensile component.

Radiation patterns may be computed from the moment tensor by contracting it with the ray strain tensor (e.g. Chapman and Leaney, 2012). The ray strain tensor, $\boldsymbol{E}$, is obtained from the dyadic of the phase slowness vector $\hat{\boldsymbol{p}}$ and polarization vector $\hat{\boldsymbol{u}}$, for the ray emanating from the source as $\boldsymbol{E} = (\hat{\boldsymbol{p}}\hat{\boldsymbol{u}} + \hat{\boldsymbol{u}}\hat{\boldsymbol{p}})/2$. This computation is approximated here using a VTI background medium, even though the focal region around the source may be of lower symmetry (orthorhombic for $\boldsymbol{M}_{planar}$ and triclinic for $\boldsymbol{M}_{rough}$). Figure 2 shows equal- area focal sphere P radiation patterns for $\boldsymbol{M}_{planar}$ and $\boldsymbol{M}_{rough}$ including homogenous VTI Green function and plotted versus VTI group angle. Nodal directions are no longer zero (middle green colour) and an asymmetry is present. It is interesting that in addition to a positive opening angle, the chosen fracture excess compliance matrix produces a rake angle of about 7° for $\boldsymbol{M}_{rough}$. More work on radiation patterns, parameter sensitivities, etc. is in the works.

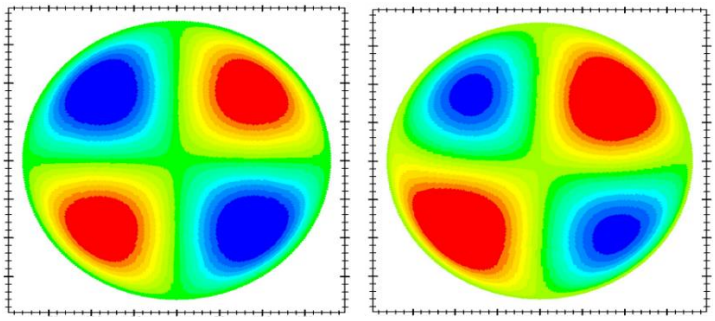

Figure 2. Equal-area P radiation patterns plotted versus VTI group angle and including homogeneous VTI Green function. Left: $\boldsymbol{M}_{planar}$, right: $\boldsymbol{M}_{rough}$.

Conclusions

The effect of fracture roughness has been included in moment tensor modelling through the inclusion of coupled excess compliances of an embedded fracture. Linear slip theory forms the foundation to create the long-wavelength-equivalent, effective fractured medium. Sources with pure slip in the fracture plane of this medium emanate tensile components due to fracture roughness as quantified by compliance coupling parameters. We conjecture that some of the tensile components observed may be explained by slip on a fault or fracture surface with roughness.

Acknowledgements

Thanks go to Chris Chapman, Václav Vavryčuk, Jim Rutledge, Colin Sayers and Edan Gofer for many helpful communications.

References

Bakulin, A., Grechka, V. and Tsvankin, I., 2000, Estimation of fracture parameters from reflection seismic data – Part III: Fractured models with monoclinic symmetry: *Geophysics*, **65**, No.6, 1818-1830.

Ben-Zion, Y., 2001, On quantification of the earthquake source: *Seismol. Res. Lett.* **72**, 151–152

Burridge, R. & Knopoff, L., 1964. Body force equivalents for seismic dislocations, *Bull. seism. Soc. Am.,* **54,** 1875–1888.

Chapman, C.H. and Leaney, W.S., 2012, A new moment-tensor decomposition for seismic events in anisotropic media: *Geophys. J. Int.*, **188**, 343-370.

Fuck, R. and Tsvankin, I., 2006, Seismic signatures of two orthogonal sets of vertical microcorrugated fractures: *Journ. Seis. Expl.*, **15**, 183-208.

Grechka, V., 2020, Moment tensors of double-couple microseismic sources in anisotropic formations: *Geophysics*, **85**, No.1, KS1-KS11.

Grechka, V. and Tsvankin, I., 2003, Feasibility of seismic characterization of multiple fracture sets: *Geophysics*, **68**, No.4, 1399-1407.

Grechka, V., Bakulin, A. and Tsvankin, I., 2003, Seismic characterization of vertical fractures described as general linear-slip interfaces: *Geophys. Prosp.*, **51**, 117-129.

Grechka, V., Li, Z., Howell, B. and Vavryčuk, V., 2017, Single-well moment tensor inversion of tensile microseismic events: *SEG Expanded Abstracts.*

Hood, J.A., 1991, A simple method of decomposing fracture-induced anisotropy: *Geophysics*, **56**, No.8, 1275-1279.

Hood, J.A. and Schoenberg, M., 1995, Decomposition of monoclinic media: Chapter 8 in *Advances in anisotropy*, SEG.

Leaney, W.S. and Chapman, C.H., 2010, Microseismic sources in anisotropic media: *EAGE Extended Abstracts*.

Leaney, W.S., 2014, *Microseismic source inversion in anisotropic media*: Ph.D. Thesis, University of British Columbia.

Minato, S., Wapenaar, K. and Ghose, R., 2020, Elastic least-squares migration for quantitative reflection imaging of fracture compliances: *Geophysics*, **85**, No.6, S337-S342.

Nakagawa, S., Nihei, K.T., Myer, L.R, 2000, Shear-induced conversion of seismic waves across single fractures: *Int. Journ. Rock Mech. Mining Sci.*, 37, 203-218.

Schoenberg, M., 1980, Elastic wave behavior across linear slip interfaces: *J. Acoust. Soc. Am.*, **68**, 1516–1521.

Schoenberg, M. and Douma, J., 1988, Elastic wave propagation in media with parallel fractures and aligned cracks: *Geophys. Prosp.*, 36, 571-590.

Schoenberg, M. and Helbig, K., 1997, orthorhombic media: Modeling elastic wave behavior in a vertically fractured earth: *Geophysics*, **62**, No. 6, 1954-1974.

Schoenberg, M., and Sayers, C., 1995, Seismic anisotropy of fractured rock: *Geophysics*, **60**, 204–211.

Vavryčuk, V., 2005, Focal mechanisms in anisotropic media: *Geophys. J. Int*., 161, 334-346.

Vavryčuk, V., 2011, Detection of high-frequency tensile vibrations of a fault during shear rupturing: observation from the 2008 West Bohemia swarm: *Geophys. J. Int.*, **186**, 1404-1414.